Exploitation of Symmetrical Non-Convexity for Symbol-Level DFRC Signal Design

Ly V. Nguyen, Rang Liu, and A. Lee Swindlehurst Center for Pervasive Communications and Computing, University of California, Irvine, CA, USA Email: vanln1@uci.edu, rangl2@uci.edu, swindle@uci.edu

Abstract—Constructive interference exploited by symbol-level (SL) signal processing is a promising solution for addressing the inherent interference problem in dual-functional radarcommunication (DFRC) signal designs. This paper considers an SL-DFRC signal design problem which maximizes the radar performance under communication performance constraints. We exploit the symmetrical non-convexity property of the communication-independent radar sensing metric to develop lowcomplexity yet efficient algorithms. We first propose a radar-to-DFRC (R2DFRC) algorithm that relies on the non-convexity of the radar sensing metric to find a set of radar-only solutions. Based on these solutions, we further exploit the symmetrical property of the radar sensing metric to efficiently design the DFRC signal. Since the radar sensing metric is independent of the communication channel and data symbols, the set of radar-only solutions can be constructed offline, therefore reducing the computational complexity. We then develop an accelerated R2DFRC algorithm that further reduces the complexity. Finally, we demonstrate the superiority of the proposed algorithms compared to existing methods in terms of both radar sensing and communication performance as well as computational complexity.

I. INTRODUCTION

Dual-functional radar communication (DFRC) [1]–[3], also often referred to as integrated sensing and communication (ISAC), is an emerging technology envisioned as a critical component of future wireless networks, e.g., 6G networks. DFRC enables both radar sensing and communication functionalities while sharing the same spectrum and transmit waveform. Therefore, DFRC can substantially improve spectral efficiency and reduce system cost and power consumption.

Due to its enormous potential, DFRC has been a subject of intense study in recent years. As an early work on DFRC, the authors in [1] proposed a radar-centric DFRC approach, which gives full priority to the radar sensing performance while treating the communication as an add-on capability accomplished by modulating the communication bits onto the radar sidelobes. Some other radar-centric methods based on index modulation were developed in [4], [5]. Since radar-centric designs completely prioritize the radar performance, they can only give limited data transmission rates.

A more common DFRC design methodology is to pursue a tradeoff between the radar sensing and communication performance. Different radar sensing and communication metrics have been considered in the literature to design DFRC signals that can balance the desired radar-communication performance.

This work was supported by the National Science Foundation under grant CCF-2008724.

For example, the studies in [3], [6]-[9] focus on maximizing the radar performance under communication constraints. The methods in [3], [6], [8] maximize the similarity between the transmit beampattern and a desired one under communication signal-to-interference-plus-noise (SINR) constraints, while the work in [7] maximizes the received radar SINR with constraints on the communication detection error probability. In [9], the Cramér-Rao bound (CRB) for the target's direction of arrival (DoA) estimate is minimized for certain communication SINR requirements. The works in [10]-[12] follow a different design perspective that optimizes the communication performance under radar constraints. For example, the communication sum rate is maximized under a beampattern similarity constraint in [10], [11], while the approach in [12] minimizes the squared error between the transmit and desired data symbols with DoA estimation CRB constraints. Instead of setting constraints on either the radar or communication performance, a weighted sum of radar and communication metrics was considered in [2], [13],

In the aforementioned works, the DFRC signals were designed via block-level (BL) processing where interference is considered as a negative factor. Rather than trying to eliminate the interference, symbol-level (SL) signal processing [15], [16] exploits interference to improve the performance of multiuser communication systems. The same idea can be applied to DFRC systems where interference from the radar signal part be exploited for the communication design. It has been shown in [17] that the SL-DFRC approach can provide significant gains compared to BL-DFRC. The authors in [17] proposed two SL-DFRC approaches, referred to as PDD-MM-BCD and ALM-RBFGS, respectively. While the PDD-MM-BCD approach relies on penalty dual decomposition (PDD), majorization-minimization (MM), and block coordinate descent (BCD), the ALM-RBFGS approach exploits the augmented Lagrangian method (ALM) and the Riemannian Broyden-Fletcher-Goldfarb-Shanno (RBFGS) algorithm. A similar design problem was studied in [18] where the linearized alternating direction method of multipliers (LADMM) algorithm was used. While the complexity of the ALM-RBFGS and LADMM approaches are lower than that of PDD-MM-BCD, they perform worse than PDD-MM-BCD.

Although PDD-MM-BCD is efficient and gives the best performance among existing work, its computational complexity is very high, scaling up to the 4th order of the number of transmit antennas. Motivated by this, in this paper, we propose low-complexity yet efficient algorithms where we exploit the symmetrical non-convexity property of the communicationindependent radar sensing metric. Our contributions are summarized as follows:

- We first propose a radar-to-DFRC (R2DFRC) algorithm that relies on the non-convexity of the radar sensing metric to find a set of radar-only solutions. Based on these solutions we further exploit the symmetrical property of the radar sensing metric to efficiently design the DFRC signal. Since the radar sensing metric is independent of the communication channel and data symbols, the set of radaronly solutions can be constructed offline, thereby reducing the computational complexity.
- We then develop an accelerated R2DFRC algorithm, hereafter referred to as aR2DFRC, that further reduces the complexity. We also analytically show that the computational complexity of the proposed R2DFRC and aR2DFRC algorithms are significantly lower than that of other existing approaches. Finally, we demonstrate that the proposed algorithms provide better performance compared to existing approaches in terms of both radar sensing and communication performance while maintaining a lower computational complexity.

II. SYSTEM MODEL AND PROBLEM FORMULATION

A. System Model

We consider a co-located monostatic multiple-input-multiple-output (MIMO) DFRC system where a BS is equipped with N antennas in a uniform linear array (ULA). The BS simultaneously serves $K_{\rm u}$ single-antenna communication users and detects the locations of $K_{\rm t}$ targets, where it is assumed that $K_{\rm u} \leq N$ and $K_{\rm t} \leq N$.

Let $\mathbf{H} = [\mathbf{h}_1, \dots, \mathbf{h}_{K_{\mathrm{u}}}]^H \in \mathbb{C}^{K_{\mathrm{u}} \times N}$ denote the downlink channel from the BS to the users. The signal vector received by the users is given as $\mathbf{y}_{\mathrm{u}} = \mathbf{H}\mathbf{x} + \mathbf{n}_{\mathrm{u}}$, where $\mathbf{x} = [x_1, \dots, x_N]^T$ is the transmit DFRC signal and $\mathbf{n}_{\mathrm{u}} \sim \mathcal{CN}(\mathbf{0}, \sigma^2 \mathbf{I}_{K_{\mathrm{u}}})$ denotes the noise at the users. We also assume that the elements of \mathbf{x} have the same constant modulus $|x_n|^2 = P/N$ for $n = 1, \dots, N$, where P is the total transmit power. In practice, the constant-modulus constraint allows the antennas to transmit at their maximum power to achieve the highest power efficiency and also guarantees low peak-to-average power ratio (PAPR), which enables the use of low-cost non-linear amplifiers.

B. Communication Performance Metric

Let $\mathbf{s} \in \mathcal{S}^{K_{\mathbf{u}}}$ denote the symbols we intend the users to detect where \mathcal{S} is the signal space. We assume D-PSK signaling, i.e., $s_k \in \mathcal{S} = \exp\left(j\pi\frac{2u_k+1}{D}\right)$ where $u_k \in \{0,\ldots,D-1\}$. Let $z_k = s_k^* \mathbf{h}_k^H \mathbf{x}$ denote the rotated noiseless received signal of user-k. The safety margin of z_k is illustrated in Fig. 1 and is defined as follows [19]:

$$\delta_k = \Re\{z_k\}\sin(\theta) - |\Im\{z_k\}|\cos(\theta),\tag{1}$$

where $\theta = \pi/D$. It is clear that the farther z_k is from the symbol decision boundaries, the more likely that the received

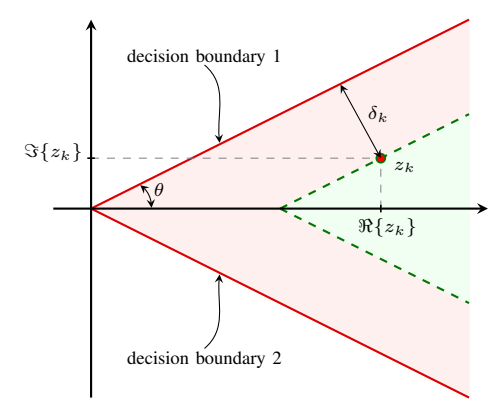


Fig. 1: Illustration of the safety margin δ_k of user-k, where $z_k = s_k^* \mathbf{h}_k^H \mathbf{x}$ is the rotated noiseless received signal of user-k.

signal $y_{u,k}$ will be correctly detected, i.e., the more robust it will be against the effects of noise and interference.

C. Radar Sensing Performance Metric

To evaluate the radar sensing performance, we consider a metric defined as the squared error between the actual and designed beampatterns. For notational convenience, let $b_\ell \stackrel{\Delta}{=} b(\vartheta_\ell)$ and $\mathbf{a}_\ell \stackrel{\Delta}{=} \mathbf{a}(\vartheta_\ell)$ respectively represent the desired beampattern and the steering vector at angle ϑ_ℓ . Consider L angles $\{\vartheta_1,\ldots,\vartheta_L\}$, the radar performance metric is given as [17]

$$f(\beta, \mathbf{x}) = \frac{1}{L} \sum_{\ell=1}^{L} |\beta b_{\ell} - \mathbf{x}^{H} \mathbf{a}_{\ell} \mathbf{a}_{\ell}^{H} \mathbf{x}|^{2},$$
 (2)

where β is a scaling parameter. Since $f(\beta, \mathbf{x})$ is a quadratic function of β , the optimal β that minimizes $f(\beta, \mathbf{x})$ is

$$\beta = \frac{\mathbf{x}^H \sum_{\ell=1}^L b_\ell \mathbf{a}_\ell \mathbf{a}_\ell^H \mathbf{x}}{\sum_{\ell=1}^L b_\ell^2}.$$
 (3)

Therefore, $f(\beta, \mathbf{x})$ can be written as

$$f(\mathbf{x}) = \sum_{\ell=1}^{L} |\mathbf{x}^H \mathbf{A}_{\ell} \mathbf{x}|^2 \text{ where } \mathbf{A}_{\ell} \stackrel{\triangle}{=} \frac{b_{\ell} \sum_{i=1}^{L} b_i \mathbf{a}_i \mathbf{a}_i^H}{\sqrt{L} \sum_{i=1}^{L} b_i^2} - \frac{\mathbf{a}_{\ell} \mathbf{a}_{\ell}^H}{\sqrt{L}}.$$

It can be seen that A_{ℓ} satisfies $A_{\ell} = A_{\ell}^{H}$, but it is not necessarily a positive semi-definite matrix.

D. Problem Formulation

We consider the problem of maximizing the radar performance under communication performance and transmit power constraints as follows:

minimize
$$\sum_{\ell=1}^{L} |\mathbf{x}^{H} \mathbf{A}_{\ell} \mathbf{x}|^{2}$$
subject to $\delta_{k} \geq \gamma_{k}, \ k = 1, \dots, K_{u},$
$$|x_{n}|^{2} = P/N, \ n = 1, \dots, N.$$
 (4)

Hence, we try to maximize the radar beampattern similarity by minimizing the difference between the designed transmit beampattern and a desired one, while guaranteeing that the safety margin δ_k of user-k is larger than or equal to a threshold γ_k .

III. PROPOSED R2DFRC METHOD

Before presenting details of the proposed R2DFRC method, we first give some important remarks about the radar objective function $f(\mathbf{x}) = \sum_{\ell=1}^L |\mathbf{x}^H \mathbf{A}_\ell \mathbf{x}|^2$ based on which we will explain our idea and develop our algorithms.

- Remark 1: $f(\mathbf{x})$ is a quartic function of \mathbf{x} , which is non-convex and therefore it has many local minima.
- Remark 2: $f(\mathbf{x})$ does not depend on the communication channel \mathbf{H} and the users' data symbols \mathbf{s} .
- Remark 3: A common phase shift to the transmit signal vector \mathbf{x} does not change the radar performance, i.e., $f(\mathbf{x}) = f(e^{j\varphi}\mathbf{x}) \ \forall \varphi$.

Our idea is to first find a set of M local radar-only solutions $\mathcal{X}^{\mathrm{R}} = \{\mathbf{x}_{1}^{\mathrm{R}}, \ldots, \mathbf{x}_{M}^{\mathrm{R}}\}$, which can be achieved easily due to Remark 1 and can also be constructed offline due to Remark 2. Then, for each radar-only solution $\mathbf{x}_{m}^{\mathrm{R}} \in \mathcal{X}^{\mathrm{R}}$, we exploit Remark 3 to efficiently find a DFRC solution $\mathbf{x}_{m}^{\mathrm{RC}}$ that satisfies the communication constraints. Finally, among the M DFRC solutions $\{\mathbf{x}_{1}^{\mathrm{RC}}, \ldots, \mathbf{x}_{M}^{\mathrm{RC}}\}$, we choose the one that gives the best radar performance as the final DFRC transmit signal design \mathbf{x}^{RC} . We use the superscripts $^{\mathrm{R}}$ and $^{\mathrm{RC}}$ to indicate 'radar-only' and 'radar-communication', respectively. In the remainder of the paper, we use the term 'radar solution' in lieu of 'radar-only solution' for brevity. Details of our proposed R2DFRC method are presented below.

A. Construction of \mathcal{X}^{R}

The radar problem is given as follows:

minimize
$$\sum_{\ell=1}^{L} |\mathbf{x}^{H} \mathbf{A}_{\ell} \mathbf{x}|^{2}$$
subject to $|x_{n}|^{2} = P/N, \forall n,$ (5)

which is non-convex and thus has many local solutions as mentioned earlier in Remark 1. Non-convex optimization problems with many local solutions are generally considered to be a roadblock. However, in this paper, we exploit this non-convex structure to construct the set \mathcal{X}^{R} . We first find a set of \tilde{M} random local solutions $\tilde{\mathcal{X}}^{\mathrm{R}}$, where $\tilde{M}\gg M$. Then, from $\tilde{\mathcal{X}}^{\mathrm{R}}$, we choose M solutions that give the best radar performance to obtain the set \mathcal{X}^{R} . Specifically, we start by randomly generating \tilde{M} initial radar solutions, which are then updated by moving along the opposite direction of the Riemannian gradient until convergence. This can be easily achieved since the gradient-based method guarantees convergence to local solutions. The Riemannian gradient of a function $f(\mathbf{x})$ can be obtained by projecting the Euclidean gradient $\nabla f(\mathbf{x})$ onto the tangent space of the complex unit circle as follows:

$$\nabla_{\mathrm{Rie}} f(\mathbf{x}) = \nabla f(\mathbf{x}) - \Re \left\{ \nabla f(\mathbf{x}) \odot \mathbf{x}^* \right\} \odot \mathbf{x}$$

where \odot denotes the element-wise multiplication operator and $\nabla f(\mathbf{x})$ can be computed as $\nabla f(\mathbf{x}) = 2 \sum_{\ell=1}^L \mathbf{x}^H \mathbf{A}_\ell \mathbf{x} \mathbf{A}_\ell \mathbf{x}$. The search for a local radar solution is done in an iterative manner using

$$\mathbf{x}^{(i_1)} \leftarrow \sqrt{P/N} \operatorname{Proj} \left(\mathbf{x}^{(i_1-1)} - \alpha_1 \nabla_{\operatorname{Rie}} f \left(\mathbf{x}^{(i_1-1)} \right) \right)$$

where i_1 is the iteration index, α_1 is a step size and $\operatorname{Proj}(\cdot)$ is the projector function that maps its argument onto the complex unit circle, i.e., $\operatorname{Proj}(x) = e^{j \angle(x)}$. In this paper, if $\Re\{\cdot\}$ and $\operatorname{Proj}(\cdot)$ are applied to a matrix or vector, they are applied separately to every element of that matrix or vector.

Since the local radar solutions in $\tilde{\mathcal{X}}^R$ are found with random initializations, some may be identical, and even if they are not the same, they may still only differ by a complex rotation $e^{j\varphi}$ since, as indicated in Remark 3, if \mathbf{x} is a local radar solution then so is $e^{j\varphi}\mathbf{x}$. Therefore, we eliminate these duplicate solutions from $\tilde{\mathcal{X}}^R$ before choosing the M best solutions to form the set \mathcal{X}^R . In our implementation, we treat any pair $\mathbf{x}_{\tilde{m}}$ and $\mathbf{x}_{\tilde{m}'}$ with $\tilde{m} \neq \tilde{m}'$ as duplicate solutions if $\mathrm{Var}(\mathrm{diag}\,(\mathbf{x}_{\tilde{m}})^{-1}\mathbf{x}_{\tilde{m}'}) \leq \epsilon$ for some small threshold ϵ , where $\mathrm{Var}(\mathbf{x})$ defines the sample variance of the elements in vector \mathbf{x} . A small threshold ϵ is used instead of 0 due to the finite precision of the data and small variations in the solutions at convergence.

B. Design of the DFRC signal \mathbf{x}^{RC}

Since the DFRC signal $x_n^{\rm RC}$ and the radar signal $x_n^{\rm R}$ both have the same constant modulus, a DFRC signal vector $\mathbf{x}^{\rm RC}$ can be written in terms of a radar solution $\mathbf{x}^{\rm R}$ as

$$\mathbf{x}^{\text{RC}} = \text{diag}(\mathbf{x}^{\text{R}})\boldsymbol{\phi},$$
 (6)

where $\phi_n = e^{j\varphi_n}$ with $\varphi_n \in [0,2\pi]$ for all n. Thus, given a radar solution \mathbf{x}^R , the design of \mathbf{x}^{RC} is equivalent to the design of the vector of rotations $\boldsymbol{\phi}$, which can be found to help make \mathbf{x}^{RC} satisfy the communication constraints. To avoid adversely affecting the radar performance, we propose to decompose $\boldsymbol{\phi}$ into two components as follows:

$$\phi = e^{j\varphi}\tilde{\phi},\tag{7}$$

where $\tilde{\phi}$ is expected to be as close as possible to $\mathbf{1}_N$. If $\tilde{\phi} = \mathbf{1}_N$, then the DFRC signal in (6) will have the same radar performance as \mathbf{x}^R due to Remark 3. Thus, the basic idea of our algorithm presented next is to design φ and a vector $\tilde{\phi}$ close to $\mathbf{1}_N$ to try to satisfy the communication constraints. The steps of the algorithm are outlined below.

1) Optimize φ for a given $\tilde{\phi}$: Using the decomposition in (7), the DFRC signal \mathbf{x}^{RC} can be written as

$$\mathbf{x}^{\mathrm{RC}} = e^{j\varphi} \operatorname{diag}(\mathbf{x}^{\mathrm{R}}) \tilde{\boldsymbol{\phi}}.$$

The rotated noiseless received signal is then given as

$$\mathbf{z} = \operatorname{diag}(\mathbf{s}^*)\mathbf{H}\mathbf{x}^{\mathrm{RC}} = e^{j\varphi}\mathbf{Q}\tilde{\boldsymbol{\phi}} = e^{j\varphi}\tilde{\mathbf{s}},$$

where $\mathbf{Q} = \mathrm{diag}\left(\mathbf{s}^*\right)\mathbf{H}\,\mathrm{diag}\left(\mathbf{x}^{\mathrm{R}}\right)$ and $\mathbf{\tilde{s}} = \mathbf{Q}\mathbf{\tilde{\phi}}$.

Let $\tilde{\mathbf{s}} = [\tilde{s}_1, \ldots, \tilde{s}_{K_{\mathrm{u}}}]^T$. The safety margin of user-k can be written as a function of φ as follows:

$$\delta_k(\varphi) = \Re\{e^{j\varphi}\tilde{s}_k\}\sin(\theta) - |\Im\{e^{j\varphi}\tilde{s}_k\}|\cos(\theta). \tag{8}$$

Since the communication constraints are $\delta_k \geq \gamma_k$, our objective will be to find an angle φ such that $\min_k \left(\delta_k(\varphi) - \gamma_k\right)$ is maximized. If φ can make $\min_k \left(\delta_k(\varphi) - \gamma_k\right) \geq 0$, then the

communication constraints are satisfied. Hence, we need to solve the following optimization problem:

$$\underset{0 \le \varphi \le 2\pi}{\text{maximize}} \quad \underset{k}{\text{min}} \ \left(\delta_k(\varphi) - \gamma_k \right). \tag{9}$$

This is a non-convex problem but it can be solved easily since it involves a single variable φ constrained in $[0, 2\pi]$. We propose an efficient algorithm to solve (9) as follows.

First, we uniformly sample the range $[0, 2\pi]$ to obtain C angle samples $\{\check{\varphi}_1, \ldots, \check{\varphi}_C\}$, i.e., $\check{\varphi}_c = 2\pi(c-1)/(C-1)$. Then, a coarse solution of φ can be found as the one in $\{\check{\varphi}_1,\ldots,\check{\varphi}_C\}$ that gives the largest $\min_k (\delta_k(\check{\varphi}_c) - \gamma_k)$, i.e.,

$$\varphi^{\text{coarse}} = \underset{\{\check{\varphi}_c\}}{\text{arg max}} \min_{k} \left(\delta_k(\check{\varphi}_c) - \gamma_k \right). \tag{10}$$

Next, starting from the coarse solution φ^{coarse} , a fine solution $\varphi^{\text{fine},(i_2)}$ at an iteration i_2 can be obtained by moving along the gradient direction until convergence:

$$\varphi^{\text{fine},(i_2)} \leftarrow \varphi^{\text{fine},(i_2-1)} + \alpha_2 \frac{\partial \delta_{\bar{k}}(\varphi^{\text{fine},(i_2-1)})}{\partial \varphi},$$
(11)

where α_2 is a step size, \bar{k} is the user index for which $\bar{k}=$ $\arg\min_{k} \left(\delta_{k}(\varphi^{\text{fine},(i-1)}) - \gamma_{k} \right)$, and the gradient is given as

$$\begin{split} \frac{\partial \delta_{\bar{k}}(\varphi)}{\partial \varphi} &= (-\sin(\varphi)\Re\{\tilde{s}_{\bar{k}}\} - \cos(\varphi)\Im\{\tilde{s}_{\bar{k}}\})\sin(\theta) - \\ &\frac{\cos(\varphi)\Im\{\tilde{s}_{\bar{k}}\} + \sin(\varphi)\Re\{\tilde{s}_{\bar{k}}\}}{|\cos(\varphi)\Im\{\tilde{s}_{\bar{k}}\} + \sin(\varphi)\Re\{\tilde{s}_{\bar{k}}\}|} \times \\ &(-\sin(\varphi)\Im\{\tilde{s}_{\bar{k}}\} + \cos(\varphi)\Re\{\tilde{s}_{\bar{k}}\})\cos(\theta). \end{split}$$

We choose to find φ_{fine} from the coarse solution in (10) instead of directly from a random sample in $[0, 2\pi]$ because the objective function in (9) is non-convex. Directly moving along the gradient direction from a random sample in $[0, 2\pi]$ will likely lead to a local solution.

2) Update
$$\tilde{\phi}$$
 for a given φ : Let $\mathbf{Q} = [\mathbf{q}_1, \dots, \mathbf{q}_K]^H$ and $\mathbf{g}_{2k} = e^{-j\varphi}\mathbf{q}_k [\sin(\theta) + e^{j\pi/2}\cos(\theta)]$

$$\mathbf{g}_{2k-1} = e^{-j\varphi} \mathbf{q}_k \left[\sin(\theta) - e^{j\pi/2} \cos(\theta) \right].$$

Then the constraint $\delta_k \geq \gamma_k$ is equivalent to the following two conditions:

$$\Re\{\mathbf{g}_{2k}^H \tilde{\boldsymbol{\phi}}\} \ge \gamma_k \tag{12}$$

$$\Re\left\{\mathbf{g}_{2k-1}^{H}\tilde{\boldsymbol{\phi}}\right\} \ge \gamma_k. \tag{13}$$

Here, $\Re\{\mathbf{g}_{2k}^H \tilde{\phi}\}$ and $\Re\{\mathbf{g}_{2k-1}^H \tilde{\phi}\}$ are the margins to the decision boundaries 1 and 2 in Fig. 1, respectively.

Consider a function of $\tilde{\phi}$ as follows:

$$\xi_{k'}(\tilde{\boldsymbol{\phi}}) = \Re\{\mathbf{g}_{k'}^H \tilde{\boldsymbol{\phi}}\} - \tilde{\gamma}_{k'},\tag{14}$$

where $k'=1,\ldots,2K_{\mathrm{u}}$ and $\tilde{\gamma}_{k'}=\gamma_k$ if k'=2k or k' = 2k - 1. We need to achieve $\min_{k'} \xi_{k'}(\hat{\phi}) \geq 0$ because the two conditions (12) and (13) are satisfied for all k when $\min_{k'} \xi_{k'}(\tilde{\phi}) \geq 0$. Therefore, we update $\tilde{\phi}$ by moving along the Riemannian gradient of the function $\xi_{\bar{k}}(\hat{\phi})$ where

$$\bar{k} = \underset{k'=1,\dots,2K_{\mathrm{u}}}{\arg\min} \, \xi_{k'}(\tilde{\boldsymbol{\phi}}).$$

Algorithm 1: Proposed R2DFRC.

```
Input: \mathcal{X}^{R}, H, and s
Output: xRC
   1: for m=1,\ldots,M do
             Initialize \phi_m = \mathbf{1}_N
   2:
  3:
              while constraints \delta_k \geq \gamma_k are not satisfied \forall k do
                  Find \varphi_m^{\text{coarse}} by (10) then set \varphi_m^{\text{fine}} = \varphi_m^{\text{coarse}}
Update \varphi_m^{\text{fine}} by (11) until convergence
Set \varphi_m = \varphi_m^{\text{fine}}
   4:
   5:
   6:
   7:
                   If \delta_k \geq \gamma_k \ \forall k, then exit the while loop
                   Update \tilde{\phi}_m by (15)
  9:
                   If \delta_k \geq \gamma_k \ \forall k, then exit the while loop
              end while
 10:
             Set \mathbf{x}_m^{\mathrm{RC}} = e^{j\varphi_m} \operatorname{diag}(\mathbf{x}_m^{\mathrm{R}}) \tilde{\boldsymbol{\phi}}_m
 13: return \mathbf{x}^{\mathrm{RC}} = \arg\min_{\{\mathbf{x}^{\mathrm{RC}}\}} f(\mathbf{x}^{\mathrm{RC}}_m)
```

The Riemannian gradient of $\xi_{\bar{k}}(\tilde{\phi})$ is given as

$$\nabla_{\mathrm{Rie}} \; \xi_{\bar{k}}(\tilde{\boldsymbol{\phi}}) = \mathbf{g}_{\bar{k}} - \Re \left\{ \mathbf{g}_{\bar{k}} \odot \tilde{\boldsymbol{\phi}}^* \right\} \odot \tilde{\boldsymbol{\phi}},$$

and thus an update of $ilde{\phi}^{(i_3)}$ can be obtained as follows:

$$\tilde{\boldsymbol{\phi}}^{(i_3)} \leftarrow \operatorname{Proj}\left(\tilde{\boldsymbol{\phi}}^{(i_3-1)} + \alpha_3 \nabla_{\operatorname{Rie}} \, \xi_{\bar{k}}\!\left(\tilde{\boldsymbol{\phi}}^{(i_3-1)}\right)\right), \tag{15}$$

where i_3 is the iteration index, and α_3 is a given step size.

It is important to note that, for a given φ , the update of $\dot{\phi}$ in (15) is implemented only once as described in Algorithm 1, since a change in ϕ affects the radar performance while a change in φ does not. In addition, ϕ is expected to be as close to $\mathbf{1}_N$ as possible to avoid radar performance loss. Therefore, we should pursue a minimal number of updates on $\tilde{\phi}$ and maximally exploit the flexibility provided by φ . Updates for ϕ and φ are terminated as soon as the communication constraints are all satisfied. The final DFRC signal design \mathbf{x}^{RC} from Algorithm 1 is the one in $\{\mathbf{x}_1^{\mathrm{RC}}, \ldots, \mathbf{x}_M^{\mathrm{RC}}\}$ that gives the best radar performance, i.e., $\mathbf{x}^{\mathrm{RC}} = \arg\min_{\{\mathbf{x}_m^{\mathrm{RC}}\}} f(\mathbf{x}_m^{\mathrm{RC}})$.

IV. PROPOSED ACCELERATED R2DFRC

In this section, we propose the aR2DFRC algorithm to further reduce the complexity of R2DFRC. Unlike R2DFRC, which performs M alternating optimizations between φ and ϕ to obtain M DFRC candidate solutions $\{\mathbf{x}_m^{\mathrm{RC}}\}$, the proposed aR2DFRC algorithm first finds the most likely radar solution and performs the alternating optimization only for it.

Specifically, we first find $\bar{\varphi}_m$ as the solution of (9) when $ilde{oldsymbol{\phi}}_m = \mathbf{1}_N$ for all m. Then, we divide the set $\mathcal{M} = \{1, \, \dots, \, M\}$ into two disjoint subsets as follows:

$$\mathcal{M}_1 = \left\{ m \in \mathcal{M} \mid \min_{k} \left(\delta_k(\bar{\varphi}_m) - \gamma_k \right) < 0 \right\}, \quad (16)$$

$$\mathcal{M}_{1} = \left\{ m \in \mathcal{M} \mid \min_{k} \left(\delta_{k}(\bar{\varphi}_{m}) - \gamma_{k} \right) < 0 \right\}, \qquad (16)$$

$$\mathcal{M}_{2} = \left\{ m \in \mathcal{M} \mid \min_{k} \left(\delta_{k}(\bar{\varphi}_{m}) - \gamma_{k} \right) \ge 0 \right\}. \qquad (17)$$

Hence, \mathcal{M}_1 is the set of indices m whose solution $(\varphi_m, \tilde{\phi}_m) =$ $(\bar{\varphi}_m, \mathbf{1}_N)$ does not satisfy the communication constraints, while \mathcal{M}_2 is the set of indices m whose solution $(\varphi_m, \phi_m) =$

TABLE I: Computational complexity comparison where I is the number of iterations.

Algorithm	Complexity
PDD-MM-BCD [17]	$\mathcal{O}(IN^3(K_{\mathrm{u}}+N))$
ALM-RBFGS [17]	$\mathcal{O}(I(N^3 + K_{\mathrm{u}}N))$
LADMM [18]	$\mathcal{O}(I(N^3 + K_{\mathrm{u}}N))$
Proposed R2DFRC	$\mathcal{O}(IM \max(C, N)K_{\mathrm{u}})$
Proposed aR2DFRC	$\mathcal{O}(\max(MC, CI, IN)K_{\mathrm{u}})$

 $(\bar{\varphi}_m,\mathbf{1}_N)$ does. This means only the pairs $\{(\varphi_{m_1},\tilde{\phi}_{m_1})\}$ with $m_1\in\mathcal{M}_1$ need to be further updated by the alternating optimization strategy presented above. However, instead of performing the alternating optimization on $\{(\varphi_{m_1},\tilde{\phi}_{m_1})\}$ for all $m_1\in\mathcal{M}_1$, we propose to do so for only the pair $\{(\varphi_{\hat{m}_1},\tilde{\phi}_{\hat{m}_1})\}$, where

$$\hat{m}_1 = \underset{\{m_1 \in \mathcal{M}_1\}}{\operatorname{arg\,max}} \quad \min_{k} \ \left(\delta_k(\bar{\varphi}_{m_1}) - \gamma_k \right). \tag{18}$$

The intuition behind this choice is that making $\min_k \left(\delta_k(\bar{\varphi}_{m_1}) - \gamma_k \right)$ large will lead to a pair $(\bar{\varphi}_{m_1}, \mathbf{1}_N)$ that satisfies the communication constraints with a minimal number of updates on $\tilde{\phi}_{m_1}$, resulting in a minimal deviation from $\mathbf{1}_N$, and consequently a minimal radar performance loss. This observation motivates us to perform the alternating optimization for only the pair $\{(\varphi_{\hat{m}_1}, \tilde{\phi}_{\hat{m}_1})\}$ to obtain a DFRC solution

$$\mathbf{x}_{\hat{m}_1}^{\mathrm{RC}} = e^{j\varphi_{\hat{m}_1}} \operatorname{diag}(\mathbf{x}_{\hat{m}_1}^{\mathrm{R}}) \tilde{\boldsymbol{\phi}}_{\hat{m}_1}.$$

Since the solutions $(\varphi_{m_2}, \tilde{\phi}_{m_2}) = (\bar{\varphi}_{m_2}, \mathbf{1}_N)$ with $m_2 \in \mathcal{M}_2$ already satisfy the communication constraints, their DFRC solutions are given as

$$\mathbf{x}_{m_2}^{\mathrm{RC}} = e^{j\bar{\varphi}_{m_2}} \operatorname{diag}(\mathbf{x}_{m_2}^{\mathrm{R}}) \mathbf{1}_N = e^{j\bar{\varphi}_{m_2}} \mathbf{x}_{m_2}^{\mathrm{R}}.$$

The final solution of the aR2DFRC algorithm is then given as

$$\mathbf{x}^{\text{RC}} = \underset{\{\mathbf{x}_{\hat{m}_{1}}^{\text{RC}}, \mathbf{x}_{\hat{m}_{2}}^{\text{RC}}\}}{\text{arg min}} \left\{ f(\mathbf{x}_{\hat{m}_{1}}^{\text{RC}}), f(\mathbf{x}_{\hat{m}_{2}}^{\text{RC}}) \right\},$$
(19)

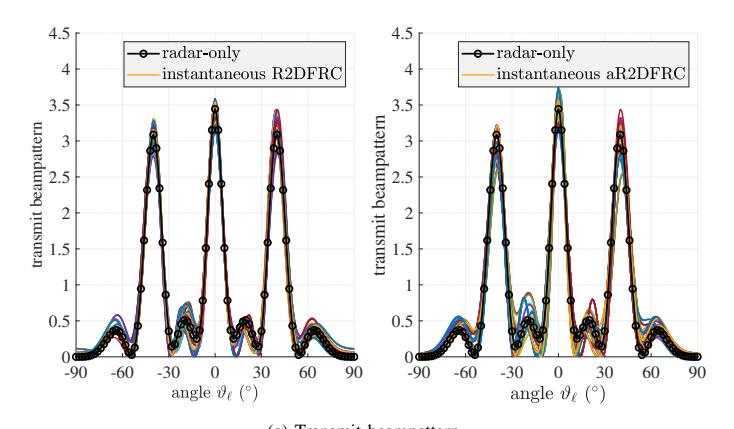
where \hat{m}_2 is the index in \mathcal{M}_2 whose DFRC solution $\mathbf{x}_{\hat{m}_2}^{\mathrm{RC}}$ gives the best radar performance among the candidates in \mathcal{M}_2 , i.e.,

$$\hat{m}_2 = \underset{\{m_2 \in \mathcal{M}_2\}}{\operatorname{arg\,min}} \quad f(\mathbf{x}_{m_2}^{\mathrm{RC}}). \tag{20}$$

V. COMPUTATIONAL COMPLEXITY ANALYSIS AND NUMERICAL RESULTS

A. Computational Complexity Analysis

A computational complexity comparison between the proposed algorithms and existing work is given in Table I. Since construction of the radar solution set \mathcal{X}^R can be performed offline, we eliminate its computational complexity from our analysis. As a result, it can be seen from Table I that the complexities of the proposed algorithms scale only linearly with the number of BS antennas N, which is significantly lower than that of the existing approaches which scale at least as N^3 . Note that the complexity of the LADMM approach in [18] scales with N^3 since each of its iterations still requires either the inversion or the eigenvalue decomposition of an $N \times N$ matrix.



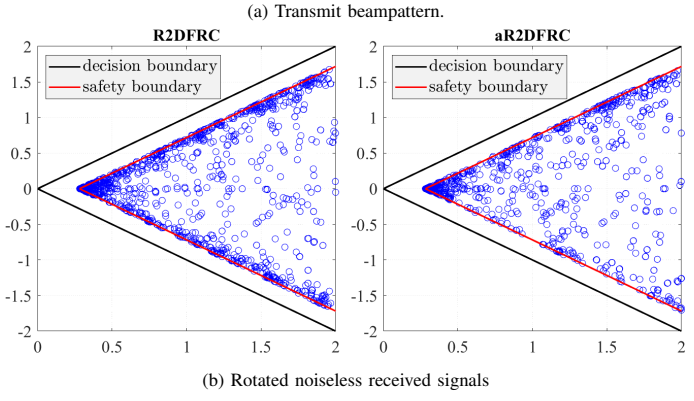


Fig. 2: Transmit beampatterns and rotated noiseless received signals by the proposed R2DFRC and aR2DFRC algorithms with $\Gamma=12$ dB.

B. Numerical Results

Here, we present numerical results to show the superiority of the proposed algorithms. We consider $K_{\rm u}=3$ users, $K_{\rm t}=3$ targets, N=10 antennas at the BS, and M=50 local radar solutions. We set $\{\vartheta_\ell\}$ to be the uniform angle samples between -90° and 90° with a resolution of 1° , where the three target angles are $\{-40^{\circ}, 0^{\circ}, 40^{\circ}\}$. The communication channels are modeled as $\mathbf{h}_k \sim \mathcal{CN}(\mathbf{0}, \zeta_k \mathbf{\Sigma}_k)$ where $\mathbf{\Sigma}_k$ is the correlation matrix and $\zeta_k = \zeta_0 d_k^{-\eta}$ is the large-scale fading coefficient. We set $\zeta_0 = -30$ dB as the reference path loss and $\eta = 2.6$ as the path loss exponent. The distance d_k between user-k and the BS is randomly generated between 100 and 800m. We set the total transmit power as P = 30 dBm and assume the noise power at the users is -169 dBm/Hz for a bandwidth of 1 MHz. The transmit symbols are assumed to be QPSK and the safety margin thresholds γ_k are set to be the same for all users as $\gamma_k = \gamma = \sigma \sin(\theta) \sqrt{\Gamma}$ where Γ represents the SINR. We set the step sizes $\alpha_1 = 0.01$, $\alpha_2 = 0.001$, and $\alpha_3 = 0.005$.

First, we show the beampatterns and the rotated noiseless received signals of the proposed R2DFRC and aR2DFRC algorithms in Fig. 2. It can be seen that both R2DFRC and aR2DFRC create beampatterns that match the desired radaronly one (Fig. 2a) while at the same time guaranteeing that signals received by the users are within the required safety margins (Fig. 2b).

Next, in Fig. 3, we compare the beampattern mean squared error (MSE) defined as $\mathbb{E}[f(\mathbf{x})]$ and the communication symbol

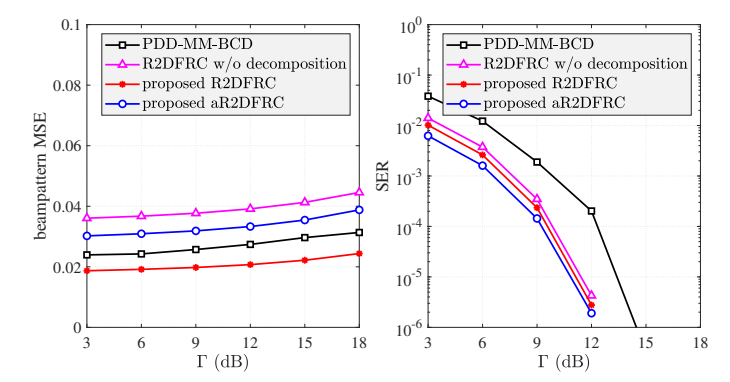


Fig. 3: Beampattern MSE and communication SER comparison.

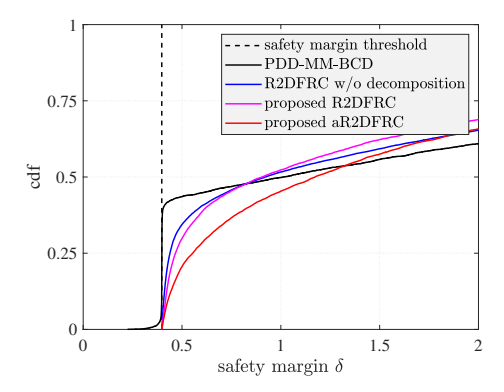


Fig. 4: Empirical cdf of safety margin at $\Gamma=15$ dB.

error rate (SER) of the proposed R2DFRC and aR2DFRC algorithms with PDD-MM-BCD in [17] and a version of R2DFRC which does not use the decomposition in (7) but uses (15) to directly find ϕ . We use PDD-MM-BCD as the benchmark since it gives the best performance among the existing approaches. It is observed from Fig. 3 that while R2DFRC gives the best performance in terms of beampattern MSE, its version without the decomposition in (7) gives the worst MSE. This verifies the effectiveness of the proposed decomposition (7), which allows exploitation of the common rotating phase φ . The MSE performance of aR2DFRC is worse than R2DFRC and PDD-MM-BCD since it only optimizes φ and ϕ for the one most likely radar candidate. However, in terms of SER, aR2DFRC gives the best performance. Both R2DFRC and aR2DFRC significantly outperform PDD-MM-BCD. This is because R2DFRC and aR2DFRC create larger safety margins while PDD-MM-BCD tends to make the users' safety margins equal the margin threshold, as can be seen in the cumulative distribution functions (cdf) in Fig. 4.

VI. CONCLUSION

In this paper, we have developed two low-complexity yet efficient SL-DFRC signal design algorithms, namely R2DFRC and aR2DFRC, which maximize the radar performance under communication safety margin constraints. We showed that the symmetrical non-convexity property of the communication-independent radar sensing metric is beneficial and can be

exploited to efficiently design the DFRC signal. We have also demonstrated the superiority of the proposed algorithms as they provide better performance in terms of both radar sensing and communication metrics while maintaining a lower computational complexity.

REFERENCES

- A. Hassanien, M. G. Amin, Y. D. Zhang, and F. Ahmad, "Dual-function radar-communications: Information embedding using sidelobe control and waveform diversity," *IEEE Trans. Signal Process.*, vol. 64, no. 8, pp. 2168–2181, Apr. 2016.
- [2] F. Liu, L. Zhou, C. Masouros, A. Li, W. Luo, and A. Petropulu, "To-ward dual-functional radar-communication systems: Optimal waveform design," *IEEE Trans. Signal Process.*, vol. 66, no. 16, pp. 4264–4279, Aug. 2018.
- [3] F. Liu, C. Masouros, A. Li, H. Sun, and L. Hanzo, "MU-MIMO communications with MIMO radar: From co-existence to joint transmission," IEEE Trans. Wireless Commun., vol. 17, no. 4, pp. 2755–2770, Apr. 2018.
- [4] T. Huang, N. Shlezinger, X. Xu, Y. Liu, and Y. C. Eldar, "MAJoRCom: A dual-function radar communication system using index modulation," *IEEE Trans. Signal Process.*, vol. 68, pp. 3423–3438, May 2020.
- [5] D. Ma, N. Shlezinger, T. Huang, Y. Liu, and Y. C. Eldar, "FRaC: FMCW-based joint radar-communications system via index modulation," *IEEE J. Select. Topics Signal Process.*, vol. 15, no. 6, pp. 1348–1364, Nov. 2021.
- [6] X. Liu, T. Huang, N. Shlezinger, Y. Liu, J. Zhou, and Y. C. Eldar, "Joint transmit beamforming for multiuser MIMO communications and MIMO radar," *IEEE Trans. Signal Process.*, vol. 68, pp. 3929–3944, June 2020.
- [7] J. Johnston, L. Venturino, E. Grossi, M. Lops, and X. Wang, "MIMO OFDM dual-function radar-communication under error rate and beampattern constraints," *IEEE J. Select. Areas Commun.*, vol. 40, no. 6, pp. 1951–1964, June 2022.
- [8] C. Qi, W. Ci, J. Zhang, and X. You, "Hybrid beamforming for millimeter wave MIMO integrated sensing and communications," *IEEE Commun. Letters*, vol. 26, no. 5, pp. 1136–1140, May 2022.
- [9] X. Wang, Z. Fei, J. A. Zhang, and J. Xu, "Partially-connected hybrid beamforming design for integrated sensing and communication systems," *IEEE Trans. Commun.*, vol. 70, no. 10, pp. 6648–6660, Oct. 2022.
- [10] Z. Cheng, Z. He, and B. Liao, "Hybrid beamforming for multi-carrier dual-function radar-communication system," *IEEE Trans. Cogn. Commun. Netw.*, vol. 7, no. 3, pp. 1002–1015, Sept. 2021.
- [11] N. T. Nguyen, L. V. Nguyen, N. Shlezinger, Y. C. Eldar, A. L. Swindlehurst, and M. Juntti, "Joint communications and sensing hybrid beamforming design via deep unfolding," arXiv:2307.04376, 2023.
- [12] Z. Cheng, S. Shi, Z. He, and B. Liao, "Transmit sequence design for dual-function radar-communication system with one-bit DACs," *IEEE Trans. Wireless Commun.*, vol. 20, no. 9, pp. 5846–5860, Sep. 2021.
- [13] Z. Cheng, Z. He, and B. Liao, "Hybrid beamforming design for OFDM dual-function radar-communication system," *IEEE J. Select. Topics Signal Process.*, vol. 15, no. 6, pp. 1455–1467, Nov. 2021.
- [14] X. Yu, Q. Yang, Z. Xiao, H. Chen, V. Havyarimana, and Z. Han, "A precoding approach for dual-functional radar-communication system with one-bit DACs," *IEEE J. Select. Areas Commun.*, vol. 40, no. 6, pp. 1965– 1977, June 2022.
- [15] C. Masouros and E. Alsusa, "Dynamic linear precoding for the exploitation of known interference in MIMO broadcast systems," *IEEE Trans. Wireless Commun.*, vol. 8, no. 3, pp. 1396–1404, Mar. 2009.
- [16] C. Masouros and G. Zheng, "Exploiting known interference as green signal power for downlink beamforming optimization," *IEEE Trans.* Signal Process., vol. 63, no. 14, pp. 3628–3640, July 2015.
- [17] R. Liu, M. Li, Q. Liu, and A. L. Swindlehurst, "Dual-functional radar-communication waveform design: A symbol-level precoding approach," *IEEE J. Select. Topics Signal Process.*, vol. 15, no. 6, pp. 1316–1331, Nov. 2021.
- [18] J. Yan and J. Zheng, "Low-complexity symbol-level precoding for dualfunctional radar-communication system," in *Proc. IEEE Wireless Commun. Netw. Conf.*, Austin, TX, USA, Apr. 2022, pp. 234–239.
- [19] H. Jedda, A. Mezghani, A. L. Swindlehurst, and J. A. Nossek, "Quantized constant envelope precoding with PSK and QAM signaling," *IEEE Trans. Wireless Commun.*, vol. 17, no. 12, pp. 8022–8034, Dec. 2018.